IEEE Access
Multidisciplinary | Rapid Review | Open Access Journal

Received September 29, 2018, accepted October 14, 2018, date of publication October 22, 2018,
date of current version November 19, 2018.

Digital Object Identifier 10.1109/ACCESS.2018.2877009

Compact Microstrip Filter With Third-Order Quasi-Elliptic Bandpass Response

JUN XU[1], FEI XIAO[1], YU CAO[2], YONG ZHANG[1], AND XIAOHONG TANG[1], (Member, IEEE)
[1]School of Electronic Science and Engineering, University of Electronic Science and Technology of China, Chengdu 611731, China
[2]Chengdu Tiger Microwave Technology Co., Ltd., Chengdu 610097, China

Corresponding author: Fei Xiao (fxiao316@outlook.com; fxiao@uestc.edu.cn).

This work was supported by the National Natural Science Foundation of China under Project 61671111.

ABSTRACT In this paper, a novel microstrip filter is proposed, which can realize a third-order quasi-elliptic bandpass response. In order to reveal the physical mechanism of the microstrip filter, a lumped-element equivalent circuit is set up and the equivalence relations between its circuit elements and the electrical parameters of the microstrip filter are presented. According to filter specifications, the initial structural parameters of the microstrip filter can be easily calculated through these equivalence relations. As demonstration, an actual microstrip filter was designed, fabricated and measured, whose center frequency is at 2.50 GHz and fractional bandwidth is 36%. There are two transmission zeros near to the passband to improve the frequency selectivity, which makes the roll-off rate at each side of the passband as high as 125 and 50 dB/GHz, respectively. The out-of-band suppression from 3.6 to 6.1 GHz is greater than 40 dB. The size of the fabricated filter is $0.21\lambda g \times 0.18\lambda g$, which is very compact.

INDEX TERMS Elliptic filter, frequency selectivity, lumped-element equivalent circuit, microstrip filter, roll-off rate, transmission zero.

I. INTRODUCTION

Up to now, various wireless applications have arisen. Efficient spectrum allocation is urgently required because spectrum resource is limited. As an important component in communication or radar systems, filter is used to let signal pass and suppress unwanted noise [1], [2]. At present, there are several types of magnitude response filters. For example, maximally-flat filters that have all their reflection zeros at the same frequency are featured by maximally-flat response. Chebyshev filters are characterized by equal ripple in passbands and their transmission zeros can be placed at finite frequencies. Elliptic filters have equal ripple in both passbands and stopbands.

In different frequency ranges, filters also have different realization forms. In low frequency range, lumped-element filters are usually used. Meanwhile, transmission-lines filters such as waveguide, coplanar waveguide and microstrip ones are widely applied in RF/microwave or even higher frequency range. For example, [3] discusses the design of hybrid folded rectangular waveguide filters with multiple transmission zeros below the passband. [4] proposes triple-mode ceramic cavity filters using the parallel-coupled resonators. Reference [5] presents a fifth-order bandpass filter based on substrate integrated waveguide with transition to grounded coplanar waveguide. In [6], bandpass filters using end-connected conductor-backed coplanar waveguide are proposed, which have controllable transmission zeros. Reference [7] presents some multilayer interdigital filters fabricated by low-temperature co-fired ceramic technology, which realize general Chebyshev filtering functions.

Compared with other transmission-line filters, microstrip filters have some advantages such as easy integration, low cost, and so on, and thus have received much attention. Until now, varieties of microstrip filters have been proposed, each of which has advantages and disadvantages and can be applied in different situation. For example, the most classic one is coupled-line microstrip bandpass filter which consists of a series of parallel-coupled two-line sections [8]. Interdigital bandpass filter consists of an array of some microstrip coupled-line sections, each of which is short-circuited at one end and open-circuited at the other end with alternative orientation [9]. Recently, [10] introduces a ultra-wideband bandpass filter in which three resonant modes are contributed by the multiple-mode resonator and four resonant modes come from a pair of electromagnetic bandgap loaded parallel-coupled lines. Reference [11] proposes a wideband

bandpass filter with composite series and shunt resonators, which creates transmission zeros on both sides of the passband. Reference [12] presents some bandpass filters based on the concept of transmission zero resonator pair, i.e., a pair of resonators with different resonant frequencies. Other microstrip filters can be found out in [4], [13]–[16]. Until now, researchers are still exploring new filter topologies with better performance.

In this paper, a novel microstrip filter is proposed, which is derived from a lumped-element bandpass filter. Appropriate microstrip counterparts are used to realize the corresponding lumped elements, and the equivalence relations between them are also presented. Thus, it's easy to understand how the desired resonances are created and coupled, and then filter design process can be greatly facilitated. The proposed microstrip filter can realize a third-order quasi-elliptic bandpass response with two transmission zeros near to the passband. In order to demonstrate it, an actual microstrip filter was designed, fabricated and measured. It's featured by good frequency selectivity and out-of-band performance. The whole paper is organized as follows: Section II presents a modified third-order lumped-element elliptic bandpass filter, in which two impedance inverters are introduced; In Section III, a novel microstrip filter with third-order quasi-elliptic bandpass response is proposed; An actual microstrip filter example is designed in Section IV; Section V discusses the experimental results; Finally, some conclusions are drawn in Section VI.

II. THIRD-ORDER LUMPED-ELEMENT ELLIPTIC BANDPASS FILTER

As one kind of transmission-line filters, the design of microstrip filters is not easy because of their distributed-element effect. In other words, the network parameters or the field components of microstrip filters usually contain complicated expressions that are not easily manipulated. In practice, it's an effective approach to apply lumped-element equivalent circuits to represent microstrip filters so that their physical mechanism can be revealed and then design process is facilitated. This paper begins with a lumped-element lowpass prototype in Fig. 1, which corresponds to a lowpass response with one transmission zero at finite frequency. Through the well-known lowpass to bandpass frequency transformation, the lumped-element bandpass filter in Fig. 2 is obtained [1]. For example, the inductors in the lowpass prototype are transformed into the series resonators, i.e.,

$$L_{ks} = \frac{R_g g_k}{W\omega_0}, \quad C_{ks} = \frac{W}{R_g \omega_0 g_k} \tag{1a}$$

where ω_0 is the center frequency, W is the factional bandwidth and R_g is the source/load resistors. The capacitors are transformed into the parallel resonators, i.e.,

$$L_{kp} = \frac{R_g W}{\omega_0 g_k}, \quad C_{kp} = \frac{g_k}{R_g \omega_0 W} \tag{1b}$$

The lumped-element bandpass filter in Fig. 2 can realize a third-order elliptic bandpass response. It has two transmission

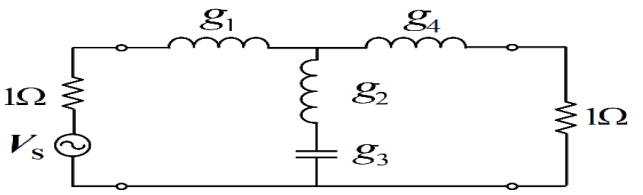

FIGURE 1. Lowpass prototype of third-order elliptic bandpass response.

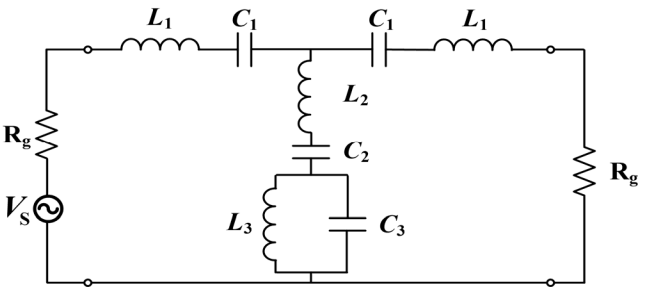

FIGURE 2. Lumped-element bandpass filter to realize a third-order elliptic bandpass response.

zeros, each of which is at different side of the passband. Obviously, it is featured by good frequency selectivity.

In order to realize it through microstrip counterparts, the filter prototype in Fig. 2 is modified. Firstly, the parallel branch is transformed, as shown in Fig. 3. In order to determine the element values of the transformed parallel branch, we can compare the input impedances of both circuits. For example, the input impedance of the left circuit is

$$Z_{in1} = sL_2 + \frac{1}{sC_2} + \frac{1}{sC_3 + \frac{1}{sL_3}} \tag{2a}$$

The input impedance of the right circuit is

$$Z_{in2} = sL_{2'} + \frac{1}{s2C_{11'} + \frac{1}{\frac{1}{s2C_{22'}} + \frac{1}{s2C_{12'} + \frac{1}{sL_{3'}}}}} \tag{2b}$$

Note that the right-handed one in Fig. 3 has five element parameters and the left-handed one has only four. In other words, there is one degree of freedom for the right-handed

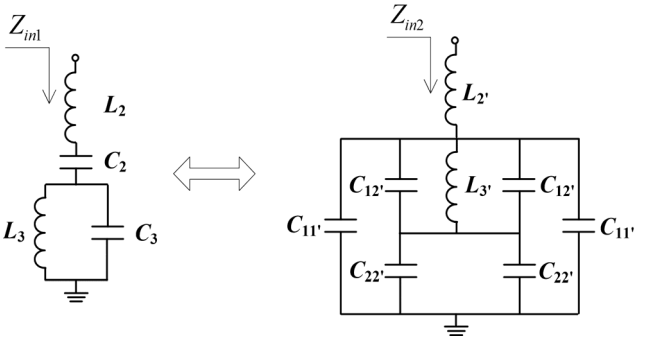

FIGURE 3. Transformation of the parallel branch.

one. Then, it's defined as Dc=$C_{11'}$-$C_{22'}$. In practice, it's flexible to adjust them so that their microstrip counterparts can meet the requirement of fabrication precision. By comparing these two input impedances, the element values of the right-handed circuit are determined from those of the left-handed one.

$$L_{2'} = L_2 \tag{3a}$$

$$L_{3'} = L_3 \frac{4C_2^2}{(Dc - C_2)^2} \tag{3b}$$

$$C_{11'} = \frac{C_2 + Dc}{4} \tag{3c}$$

$$C_{22'} = \frac{C_2 - Dc}{4} \tag{3d}$$

$$C_{12'} = -\frac{(C_2 - Dc)\left[C_2^2 + C_3 Dc + C_2 (Dc - C_3)\right]}{8C_2^2} \tag{3e}$$

In order to realize the one in Fig. 2 through microstrip, it's likely to find out appropriate microstrip counterpart for each part, and then connect them according to the schematic in Fig. 2. In reality, some parts of Fig.2 could not be realized directly. Then, it's modified as the one in Fig. 4, in which two impedance inverters are inserted. Obviously, the magnitude responses of both lumped-element bandpass filters are the same.

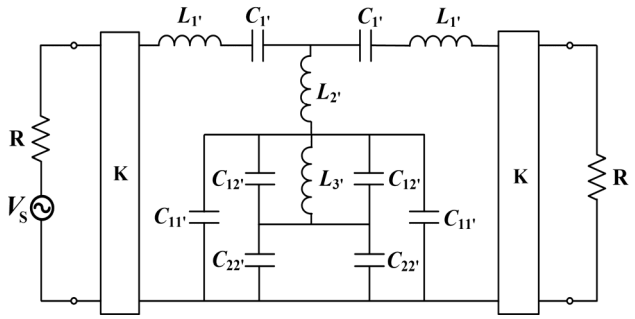

FIGURE 4. Modified lumped-element bandpass filter.

Apart from the relations described by the equations (3a)-(3e), the other element values of the modified filter in Fig. 4 are easily determined by the ones in Fig. 2. For example,

$$R_g \cdot R = K^2 \tag{4a}$$

$$L_{1'} = L_1 \tag{4b}$$

$$C_{1'} = C_1 \tag{4c}$$

III. MICROSTRP FILTER WITH THIRD-ORDER ELLIPTIC BNADPASS RESPONSE

In the previous section, a modified lumped-element filter is presented in Fig. 4. In order to realize it through microstrip, it's necessary to find out some appropriate microstrip counterparts to realize the corresponding elements of the former. In the following, some microstrip structures are discussed, and their lumped-element equivalent circuits and the equivalence relations are presented.

A. EQUIVALENT CIRCUIT OF MICROSTRIP PARALLEL-COUPLED TWO-LINE SECTION

Parallel-coupled two-line section in Fig. 5 is widely used in the construction of microstrip filters, where Z_e and Z_o are the even- and odd-mode characteristic impedances respectively, and θ is the electrical length. It can be described the following [*ABCD*] matrix, (5), as shown at the bottom of this page. However, it's not easy to directly manipulate it. Then, a lumped-element equivalent circuit in Fig. 5 is introduced to represent it, which is obtained from the one in [17]–[19] by omitting one resonance. The equivalence relations to describe the relationship between the electric parameters of the microstrip parallel-coupled two-line section and the element values of the equivalent circuit are

$$L = \frac{\pi}{8\omega_0 (Z_e + Z_o)} \tag{6a}$$

$$C = \frac{8}{\pi \omega_0 (Z_e + Z_o)} \tag{6b}$$

$$K = \frac{Z_e - Z_o}{2 \sin\theta} \tag{6c}$$

where $\omega_0 = 1/\sqrt{LC}$ is the resonant angular frequency. Here, a microstrip parallel-coupled two-line section is used to realize the impedance inverter K, the inductor $L_{1'}$ and the capacitor $C_{1'}$ in Fig. 4.

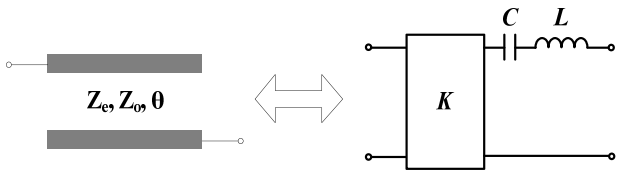

FIGURE 5. Parallel-coupled two-line section and its lumped-element equivalent circuit used in this paper.

B. MICROSTRIP REALIZATION OF THE PARALLEL BRANCH

As is well known, a short high-impedance microstrip line section is equivalent to an inductor, as shown in Fig. 6. If the impedance is chosen firstly, the electric length can be determined by the following equivalence relation.

$$\theta_H = 2 \arctan\left(\frac{\omega_0 L}{2Z_H}\right) \tag{7}$$

$$[ABCD] = \begin{bmatrix} \frac{Z_e+Z_o}{Z_e-Z_o}\cos\theta & j\frac{1}{2\sin\theta(Z_e-Z_o)}\left((Z_e-Z_o)^2-(Z_e+Z_o)^2\cos^2\theta\right) \\ j\frac{2}{Z_e-Z_o}\sin\theta & \frac{Z_e+Z_o}{Z_e-Z_o}\cos\theta \end{bmatrix} \tag{5}$$

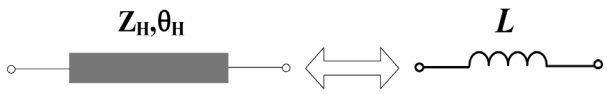

FIGURE 6. Short high-impedance microstrip line section equivalent to an inductor.

where L is the inductor value. Z_H and θ_H are the impedance and electric length of the microstrip line section respectively. ω_0 is the angular frequency where approximation is made. Here, it's set at the center frequency.

In addition, a short low-impedance open-circuited microstrip stub could be considered as a capacitor, as shown in Fig. 7. If the impedance of the microstrip stub is chosen firstly, its electric length is determined by the following equivalence relation.

$$\theta_L = \arctan(\omega_0 C Z_L) \tag{8}$$

where C is the capacitor value. Z_L and θ_L are the impedance and electric length of the microstrip stub respectively.

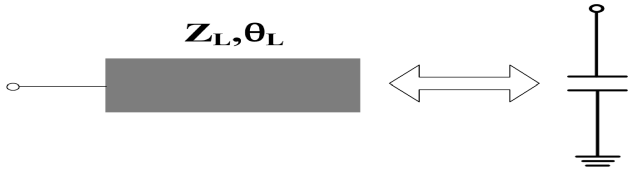

FIGURE 7. Short open-circuited low-impedance microstrip stub equivalent to an capacitor.

After understanding the equivalent circuits of these basic microstrip structures, we can construct one to realize the parallel branch in Fig. 4, i.e., the right-handed circuit in Fig. 3. It is shown in Fig. 8. For example, the microstrip line section with the impedance Z_{H1} and the electric length θ_{H1} is used to realize the inductor $L_{2'}$, and the microstrip line section with the impedance Z_{H2} and the electric length θ_{H2} is used to realize the inductor $L_{3'}$ the right-handed circuit in Fig. 3, respectively. On the other hand, the open-circuited microstrip stub with the impedance Z_{L1} and the electric length θ_{L1} is used to realize the capacitor $C_{11'}$, the open-circuited microstrip stub with the impedance Z_{L2} and the electric length θ_{L2} realizes the capacitor $C_{22'}$, the right-handed circuit in Fig. 3, respectively. Finally, the coupling between the two microstrip stubs realizes the capacitor $C_{12'}$.

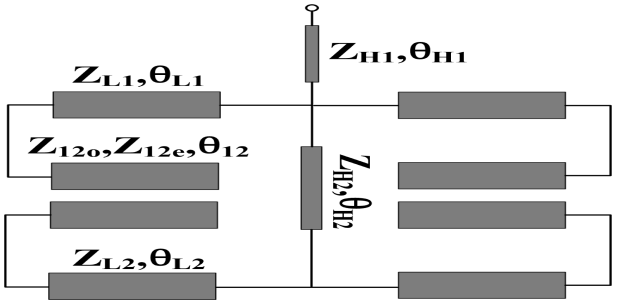

FIGURE 8. Microstrip realization of the parallel branch in Fig. 4.

C. SCHEMATIC OF MICROSTRIP FILTER

After the lumped elements of the lumped-element filter in Fig. 4 is realized through the corresponding microstrip counterparts mentioned in the previous subsections, a microstrip filter is obtained, as shown in Fig. 9.

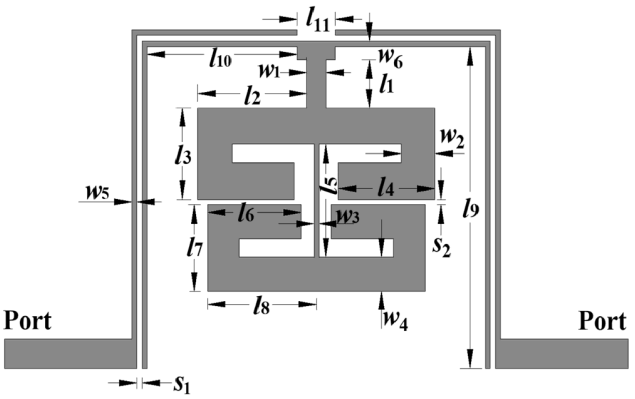

FIGURE 9. Microstrip filter proposed in this paper.

IV. MICROSTRIP FILTER DESIGN EXAMPLE

In the previous sections, how to construct the proposed microstrip filter is discussed in detail. At the same time, the physical mechanism of the proposed microstrip filter is also revealed, which is beneficial to its design. The design procedure of the proposed microstrip filter includes three steps: firstly, the lumped-element equivalent circuit in Fig. 4 should be synthesized according to filter specifications; secondly, the electrical parameters of the microstrip filter in Fig. 9 are calculated through the equivalence relations; finally, structural parameters are calculated and then act as initial values for next-step optimization. To slightly adjust the structural parameters in the vicinity of these calculated ones makes filter performance meet requirement. For convenience, it's called the distributed- to lumped-element equivalence (DLEE) method here.

For demonstration, a microstrip filter example is designed. For instance, it's used to realize an elliptic bandpass response with center frequency at 2.50 GHz and fractional bandwidth of 36%. The in-band return loss is set greater than 20 dB. One transmission zero is at 1.56 GHz and the other one at 4.04 GHz, respectively. The ideal response is shown in Fig. 10. Both source and load impedances are set as 50 Ω. In the first step of the DLEE, conventional synthesis technique is used. According to filter specifications, the lowpass prototype in Fig. 1 should be synthesized where g_1=0.7604, g_2=0.1409, g_3=0.9456 and g_4=0.7604. The lowpass response is shown in Fig. 11.

In practice, all structural parameters should meet the requirement of fabrication precision. As required by the fabrication technique we currently use, minimum line width and

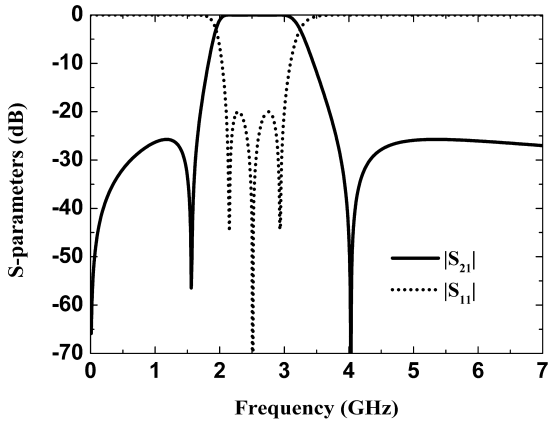

FIGURE 10. Ideal third-order elliptic bandpass response.

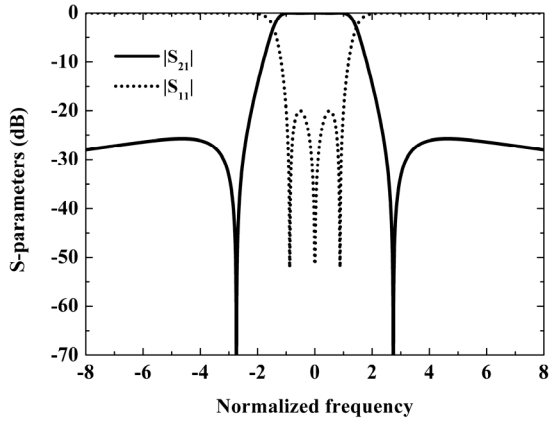

FIGURE 11. Lowpass response.

gap should not be less than 0.12 mm. For the microstrip filter in this paper, Rg and Dc should be set reasonably to make the structural parameters meet requirement. For example, Rg=36.98 Ω, and thus a set of the structural parameters satisfying our fabrication precision are determined for the parallel-coupled two-line sections. Similarly, $C_{12'}$ starts to be greater than 0 pF when Dc=-0.27 pF.

If R_g is set as 36.98 Ω, the element values in Fig. 2 are calculated through the equations (1a) to (1b), i.e., L_1=4.9722 nH, C_1 = 0.8086 pF, L_2 = 0.9213 nH, C_2 = 4.3639 pF, L_3 = 0.8892 nH and C_2 = 4.5214 pF, respectively.

If Dc is set as −0.27 pF, the element values in Fig. 4 can be determined by using the equations (3a) to (4c). For example, R = 50 Ω, K = 43 Ω, $L_{1'}$ = 4.9722 nH, $C_{1'}$ = 0.8086 pF, $L_{2'}$ = 0.9213 nH, $L_{3'}$ = 3.1544 nH, $C_{11'}$ = 1.0235 pF, $C_{22'}$ = 1.1585 pF and $C_{12'}$ = 0.0939 pF, respectively.

In the second step, the electrical parameters of the microstrip filter are calculated through the equivalence relations (6)-(8). For example, the odd- and even-mode impedances of the coupled-line two-line sections are Z_o=56.8431 Ω and Z_e=142.8413 Ω respectively, and their electric lengths are $\pi/2$ at the center frequency. If the impedance Z_{H1} is chosen as 65 Ω, the electric length θ_{H1}=12.7547°. If the impedance Z_{H2} is chosen as 110 Ω, the electric length θ_{H1}=25.4837°. If the impedance Z_{L1} is chosen as 45 Ω, the electric length θ_{L1}=35.9936°. If the impedance Z_{L2} is chosen as 45 Ω, the electric length θ_{L2}=39.4264°.

In the third step, the structural parameters of the microstrip filter can be calculated through these obtained electric parameters if an actual substrate is chosen. For example, Rogers RT/duroid 4350 substrate with a relative permittivity of 3.66 and a dielectric height of 0.508 mm is used in this paper. The initially simulated results of the microstrip filter with the calculated structural parameters are depicted in Fig. 12. The responses are close to the ideal ones in Fig. 10. For example, the passband almost covers the desired frequency range. Two transmission zeros near to the passband are clearly observed. Unfortunately, the in-band return loss does not meet requirement.

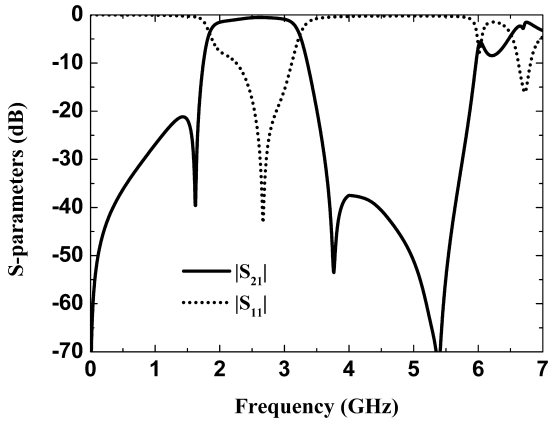

FIGURE 12. Initially simulated results of the microstrip filter with calculated structural parameters.

The analytical modeling focuses on revealing the main physical mechanism of the microstrip filter, and thus it's unlikely to include all actual factors. In order to offset some minor discontinuity effect such as loss, bend, open end and junction that are not considered in the analytical modeling, full-wave simulation should be applied to optimize the performance of the actual microstrip filter. Then, these calculated structural parameters are taken as initial values. By adjusting these structural parameters in the vicinity of the calculated ones, a set of the structural parameters with optimized performance are obtained, i.e., l_1 = 1.80 mm, l_2=4.36 mm, l_3=3.41 mm, l_4=3.81 mm, l_5=4.20 mm, l_6=3.76 mm, l_7=3.21 mm, l_8=4.26 mm, l_9=12.00 mm, l_{10}=6.00 mm, l_{11}=1.54 mm, w_1=0.78 mm, w_2=1.36 mm, w_3=0.20 mm, w_4=1.26 mm, w_5=0.20 mm, w_6=0.69 mm, s_1=0.22 mm, and s_2=0.20 mm, respectively.

In Fig. 13, the simulated responses of the microstrip filter with the optimized structural parameters are shown. Compared with the initially simulated responses in Fig. 12, the filter performance is improved to meet filter specifications.

Understanding physical mechanism of the microstrip filter is very important to controlling its performance. For example,

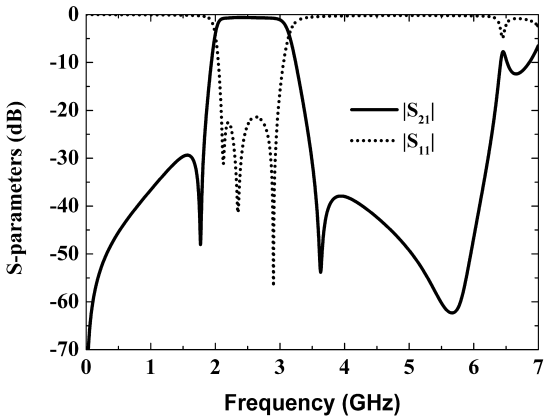

FIGURE 13. Simulated responses of the microstrip filter with optimized structural parameters.

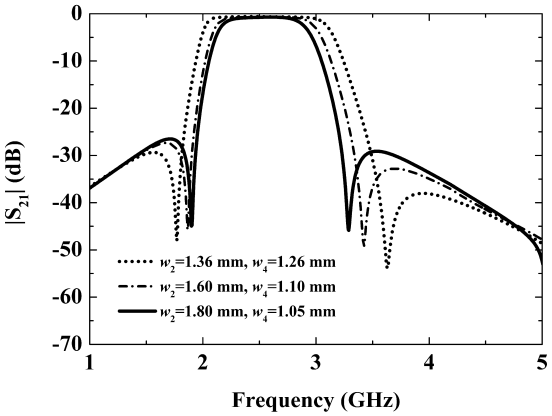

FIGURE 14. Bandwidth adjustment.

Fig. 14 illustrates how to adjust its bandwidth through changing some key structural parameters meanwhile the center frequencies are almost kept unchanged. It clearly demonstrates that the performance of the proposed microstrip filter is very flexible.

V. MEASUREMENT AND DISCUSSION

In order to verify the previous analysis, an actual microstrip filter was fabricated and measured. The photo of the fabricated filter is shown in Fig. 15. It's very compact and the size is only $0.21\lambda_g \times 0.18\lambda_g$ where λ_g is the waveguide wavelength at the center frequency. Both simulated and measured results are presented in Fig. 16, which coincide well. The measured passband can cover the desired frequency range. The insertion loss at the center frequency is only 0.59 dB, which includes the loss of a pair of SMA connectors. The in-band return loss is greater than 15 dB. There is a transmission zero at the left side of the passband so that the roll-off rate is as high as 125 dB/GHz. Simultaneously, there is another transmission zero at the right side of the passband, which obtains 50 dB/GHz roll-off rate. Undoubtedly, these two transmission zeros near to the passband greatly improve frequency selectivity. In addition, the filter is also featured by good

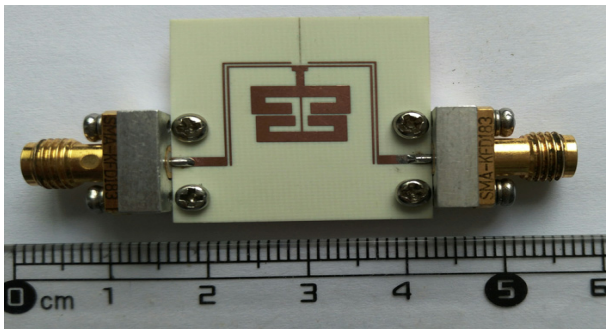

FIGURE 15. Photo of the fabricated microstrip filter.

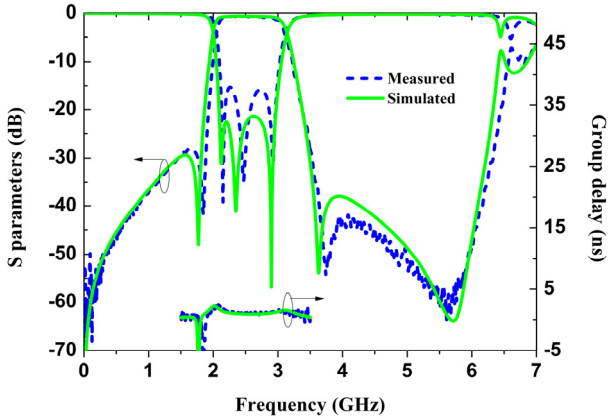

FIGURE 16. Simulated and measured results of the microstrip filter with optimized structural parameters.

TABLE 1. Performance comparison between the proposed filter and several other third-order bandpass filters.

Ref.	f_0 (GHz)	FBW (%)	RL (dB)	IL (dB)	RSB	Upper stopband (dB)	Size ($\lambda_g \times \lambda_g$)
[13]	5.00	14.0	5.0	1.1	-	14.0	0.45×0.48
[14]	2.70	16.7	21.0	0.6	0.96	12.0	0.19×0.08
[15]	3.50	16.0	10.0	1.9	-	10.0	0.25×0.38
[16]	4.67	38.0	10.0	0.7	0.26	12.8	0.73×0.73
[4]	1.84	4.1	21.0	0.4	0.16	9.0	0.57×0.57
[20]	2.00	10.0	17.0	1.7	-	31.0	0.79×0.06
This work	2.50	36.0	15.0	0.6	1	42.0	0.21×0.18

FBW: fractional bandwidth. RL: return loss. IL: insertion loss. RSB: relative stopband bandwidth described by $\Delta f/f_0$ where Δf is the stopband bandwidth. Note that some data of some filters in other literatures are estimated because they are not directly described.

out-of-band performance. More than 40 dB suppression is achieved from 3.6 to 6.1 GHz. The simulated and measured in-band group delays are also shown in Fig. 16. The variation of the measured in-band group delay is less than 1 ns.

In order to clearly demonstrate the advantages of the proposed microstrip filter, its performance is compared with that of other third-order bandpass filters in some literatures. The results are listed in Table I. Obviously, the proposed one is featured by good out-of-band performance and compact size.

VI. CONCLUSION

In this paper, a novel microstrip filter is proposed in this paper, which realizes a third-order quasi-elliptic bandpass response. With the aid of lumped-element equivalent circuit, how the resonances are created and coupled is described clearly. Understanding its physical mechanism greatly facilitate design process. Especially, the equivalence relations are presented. Thus, it's very easy to calculate the initial structural parameters of the microstrip filter according to filter specifications. As the measured results show, the proposed microstrip filter is featured by good frequency selectivity and out-of-band performance. The idea in this paper also applies to other transmission-line filters.

ACKNOWLEDGMENT

The authors would like thank Miss Rudan Xiao for her wholehearted support!

REFERENCES

[1] G. Matthaei, L. Young, and E. M. T. Jones, *Microwave Filters, Impedance-Matching Networks, and Coupling Structures*. Norwood, MA, USA: Artech House, 1980.

[2] J. S. Hong and M. J. Lancaster, *Microstrip Filters for RF/Microwave Applications*. New York, NY, USA: Wiley, 2001.

[3] C. Carceller, P. Soto, V. E. Boria, and M. Guglielmi, "Design of hybrid folded rectangular waveguide filters with transmission zeros below the passband," *IEEE Trans. Microw. Theory Techn.*, vol. 64, no. 2, pp. 475–485, Feb. 2016.

[4] D. R. Hendry and A. M. Abbosh, "Analysis of compact triple-mode ceramic cavity filters using parallel-coupled resonators approach," *IEEE Trans. Microw. Theory Techn.*, vol. 64, no. 8, pp. 2529–2537, Aug. 2016.

[5] J. Zhang, X. Zhang, D. Shen, and K. Wu, "Gap waveguide PMC packaging for a SIW-GCPW-based filter," *IEEE Microw. Wireless Compon. Lett.*, vol. 26, no. 3, pp. 159–161, Mar. 2016.

[6] J. K. Xiao, M. Zhu, J. G. Ma, and J. S. Hong, "Conductor-backed CPW bandpass filters with electromagnetic couplings," *IEEE Microw. Wireless Compon. Lett.*, vol. 26, no. 6, pp. 401–403, Jun. 2016.

[7] A. Périgaud, S. Bila, S. Verdeyme, D. Baillargeat, and D. Kaminsky, "Multilayered coupled interdigital resonator filters for general Chebyshev filtering functions," *IEEE Trans. Microw. Theory Techn.*, vol. 64, no. 5, pp. 1465–1475, May 2016.

[8] S. B. Cohn, "Parallel-coupled transmission-line-resonator filters," *IRE Trans. Microw. Theory Tech.*, vol. MTT-6, no. 2, pp. 223–231, Apr. 1958.

[9] G. L. Matthaei, "Interdigital band-pass filters," *IEEE Trans. Microw. Theory Techn.*, vol. MTT-10, no. 6, pp. 479–491, Nov. 1962.

[10] C.-X. Zhou, P.-P. Guo, K. Zhou, and W. Wu, "Design of a compact UWB filter with high selectivity and superwide stopband," *IEEE Microw. Wireless Compon. Lett.*, vol. 27, no. 7, pp. 636–638, Jul. 2017.

[11] Z. Li and K.-L. Wu, "Direct synthesis and design of wideband bandpass filter with composite series and shunt Resonators," *IEEE Trans. Microw. Theory Techn.*, vol. 65, no. 10, pp. 3789–3800, Oct. 2017.

[12] Q. Xue and J. Y. Jin, "Bandpass filters designed by transmission zero resonator pairs with proximity coupling," *IEEE Trans. Microw. Theory Techn.*, vol. 65, no. 11, pp. 4103–4110, Nov. 2017.

[13] L. Zhu and W. Menzel, "Compact microstrip bandpass filter with two transmission zeros using a stub-tapped half-wavelength line resonator," *IEEE Microw. Wireless Compon. Lett.*, vol. 13, no. 1, pp. 16–18, Jan. 2003.

[14] S. Zhang and L. Zhu, "Compact and high-selectivity microstrip bandpass filters using triple-/quad-mode stub-loaded resonators," *IEEE Microw. Wireless Compon. Lett.*, vol. 21, no. 10, pp. 522–524, Oct. 2011.

[15] H. W. Liu *et al.*, "Triple-mode bandpass filter using defected ground waveguide," *Electron. Lett.*, vol. 47, no. 6, pp. 388–389, Mar. 2011.

[16] C. Jin and Z. Shen, "Compact triple-mode filter based on quarter-mode substrate integrated waveguide," *IEEE Trans. Microw. Theory Techn.*, vol. 62, no. 1, pp. 37–45, Jan. 2014.

[17] G. L. Matthaei, "Design of parallel-coupled resonator filter," *IEEE Microw. Mag.*, vol. 8, no. 5, pp. 78–87, Oct. 2007.

[18] D. Swanson and G. Macchiarella, "Microwave filter design by synthesis and optimization," *IEEE Microw. Mag.*, vol. 8, no. 2, pp. 55–69, Apr. 2007.

[19] F. Xiao, "Microstrip band-pass filters without source/load inverters," *Int. J. Circuit Theory Appl.*, vol. 46, no. 3, pp. 415–426, Mar. 2018.

[20] C.-J. Chen, "A coupled-line coupling structure for the design of quasi-elliptic bandpass filters," *IEEE Trans. Microw. Theory Techn.*, vol. 66, no. 4, pp. 1921–1925, Apr. 2018.

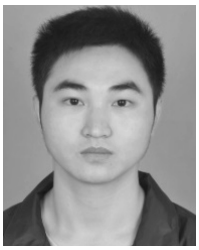

JUN XU is currently pursuing the master's degree under the supervision of Prof. F. Xiao.

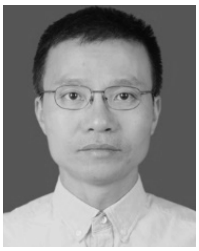

FEI XIAO received the M.Sc. and Ph.D. degrees from the University of Electronic Science and Technology of China (UESTC) in 2002 and 2005, respectively. From 2009 to 2010, he was a Visiting Researcher with the KTH Royal Institute of Technology, Sweden. From 2015 to 2016, he was a Visiting Researcher with the University of Birmingham, U.K. He is currently a Professor with UESTC. He has authored over 80 journal and conference papers and holds 14 authorized patents. His research interests include filter synthesis, microwave passive components design, and computational electromagnetics.

YU CAO received the B.S. degree from the Southwest University of Science and Technology, China, in 2006, and the M.Eng. degree from the University of Electronic Science and Technology of China, China, in 2015. Since 2015, he has been the R&D Director of the Communication BU with Chengdu Tiger Microwave Technology, Co., Ltd. His research areas include microwave/millimeter wave circuit design.

YONG ZHANG received the B.S., M.Sc., and Ph.D. degrees from the University of Electronic Science and Technology of China (UESTC), Chengdu, China, in 1999, 2001, and 2004, respectively. He was a Visiting Scholar with Harvard University and the Illinois Institute of Technology, USA, respectively. He is currently a Professor with UESTC. He has authored over 100 journal and conference papers and holds five authorized patents. His current research interests include the design and application of passive and active components at RF frequencies, and solid-state terahertz technology.

XIAOHONG TANG (M'08) received the B.S. and Ph.D. degrees in electromagnetism and microwave technology from the University of Electronic Science and Technology of China (UESTC), Chengdu, China. He is currently a Professor with UESTC. He has authored over 100 journal and conference papers. His current research interests include microwave and millimeter-wave circuits and systems, microwave integrated circuits, and computational electromagnetism.